

# Theoretical Assessment of a Hybrid Solar-Still System Via Waste Heat from Air Conditioning System Condenser

Murtadha Hamid Azeez <sup>1,\*</sup>, Salman Hashim Hammadi <sup>2</sup>

<sup>1,2</sup> Department of Mechanical Engineering, College of Engineering, University of Basrah, Basrah, Iraq

E-mail addresses: [pgs.murtadha.hamid.azeez@uobasrah.edu.iq](mailto:pgs.murtadha.hamid.azeez@uobasrah.edu.iq), [salman.hammadi@uobasrah.edu.iq](mailto:salman.hammadi@uobasrah.edu.iq)

Received: 1 July 2023; Revised: 15 September 2023; Accepted: 26 September 2023; Published: 15 February 2024

## Abstract

In this paper, a theoretical study of the conventional solar-still system integrated via the design of heat recovery of air exhausted from the air conditioner condenser employing heat exchangers (WHRUs) was conducted. This study aims to improve desalination performance by compensating for the non-existence of sunlight during the night. A comparison was made between the desalination performance in the event of exposure to solar radiation and its performance in the case of exposure to the system (WHRUs). It was found that the (WHRUs) system has a minimal impact on the production of the conventional desalination rig during the night period, as the highest cumulative productivity in the presence of the (WHRUs) reached (2.15 kg) in August. In contrast, the productivity dependent on solar radiation was (4.58 kg) for the same month, with the most significant percentage of improvement reaching (31.91 %).

**Keywords:** Solar still, Single slope, Solar desalination. Solar radiation, Waste heat recovery system.

<https://doi.org/10.33971/bjes.24.1.3>

## 1. Introduction

The world, in general, and Iraq, in particular, will face a great scarcity of drinking water due to the impending oil and gas crises, the importance of having alternatives to everything that depended on traditional energies, as well as because of the impending oil and gas crises, and the importance of having alternatives to everything that depended on conventional energies, i.e., fossil fuels, especially the issue of drinking water, because it affects human life furthermore the rapid increase in population growth. All these reasons led to the development of traditional desalination plants powered by fossil fuels and electricity for their replacement with renewable energy resources, especially solar Energy. Therefore, solar distillation technology came as a renewable technology that does not consume Energy, as it is cheap and not harmful to the environment, as is known in traditional-desalination methods.

However, the main challenge with solar-still systems was the severe weakness in performance and productivity. Some studies were conducted to convert the passive system into an active solar distiller to enhance the poor productivity of the solar distiller system. It is carried out by improving heat exchange within the system basin, supplying an external heat source on the basin's system, and incident solar-radiation energy. It was achieved by integrating the solar distillation system with solar collectors, condensers, heaters, cooling towers, solar chimneys, and other methods [1].

Rai and Tiwari [2] combined the solar collector with the single-slope solar distiller system basin. They found that the daily rate of fresh water was higher than the conventional simple distiller system by up to (24%). Another study discussed the effect of thermal model analysis of active and

solar distillation using a solar collector, depending on the concept of solar energy fraction. The researchers found R. Tripathi and Tiwari [3] that the increase in the water surface level in the system basin caused a decrease in the water temperature. Thus, the heat transfer coefficient decreased by convection, and the degree of agreement was acceptable between the experimental and analytical results.

Shawki [4] studied the efficiency of the performance of the double-slope solar distilled utilizing the evacuated tubes with heat-pipe for the atmosphere of the city of Basra, Iraq, a theoretical study and compared that study with the experimental results. The researcher used software for artificial neural networks to know the rate of productivity improvement, as well as to calculate the heat transfer and heat flux coefficients theoretically. The results showed that the crop for the first day of July 2013 was (11.3 kg) from eight to five o'clock in the evening. The efficiency rate for this period was (16.44%). The results of the composite system of (evacuated tubes with heat pipe connected to double-slope solar still) that the researcher used were compared with (conventional solar still). The result was an increase in productivity by (43.35%).

Mahammed et al. [5] presented a numerical made by connecting the solar distillation system to an external condensing room, where a heat exchanger connected them to see the effect of this condenser on the performance of the distiller. The performance of the numerical mathematical model was compared with the results of solar distillation in the condition without adding a condenser. It was concluded that the most significant monthly productivity is obtained in the middle of the summer season, especially in August, when the output was (6.7 kg/m<sup>2</sup>) at a cooling rate of (12 g/s), meaning there is an improvement in the output by (60 %) compared to the solar distillation systems that operate without condensers.

From this, the researcher concluded that productivity is sensitive to the rate of water cooling.

Abdel-Rehim and Lashen [6] modified two solar distillation systems, using in the first a compact bed of glass balls that store heat and using in the second a rotating shaft placed near the basin's water surface that is rotated by a source of photovoltaic cells (P-V) through an inverter. A comparison was made between the conventional solar distiller and the two systems modified with glass balls and rotor shafts, respectively. It was found that the two systems modified with heat-storing balls and those with a rotating shaft improved the performance, efficiency, and productivity of solar stills. In May, June, and July, the performance efficiency of the modified system with heat-storing balls showed (5 %), (6 %) and (7.5 %), respectively. As for the system with a rotating shaft connected to a (P-V) cell, the efficiency for the months mentioned above reached (2.5 %), (5 %) and (5.5 %) respectively.

Other studies of improved heat exchange within the solar distillation basin are the recovery of waste heat from machines and devices that operate with thermal Energy according to the laws of thermodynamics (from the thermal source (hot reservoir) of high temperature to the thermal sink (cold reservoir) of lower temperature, or vice versa) instead of wasting this Energy in vain scattered in the atmospheric environment. It was done through the work of a recovery system for this heat through many theoretical and practical experiments.

Kumar et al. [7] presented a model of a solar distiller combined with waste heat from a pellet-based food cooking stove to find the optimal water cap thickness and the mass rate of water flow to recover waste heat from the stove. It has been reached: First, the heat transfer increases linearly (and vice versa) by decreasing the mass flow rate of water to the lowest level, which reaches 0.055 kg/sec. Second, the thickness of the water layer should not exceed 8 mm because its height reduces the temperature of this salty water layer. Third, it can operate during daylight hours when the sun is shining, and it is suitable to meet the needs of a small family if the government supports such projects.

Shafieian and Khiadani [8] introduced a new multipurpose method for water desalination, cooling, and air conditioning by recycling waste heat from diesel engine exhausts and submarine cooling water because the dry air coming out of those exhausts has high temperatures that are thrown into the atmosphere without benefiting from it. Hence, the researchers proposed a mathematical model based on Physical variables for the fumes of those exhausts. The analysis showed that when the exhaust fumes masses are high, the water mass flow rates are high due to the high exhaust temperatures. Also, by heat transfer coefficients (0.45) and the relative mass of exhaust gas (0.37-0.53), performance coefficients (0.83-0.88) were achieved. This well-known system reduces the need for costly sources to obtain drinking water in those places where it is difficult to obtain fresh water, as in the case of submarines in the depths of the seas and oceans, and the lack of the need for excessive expenditure of fossil fuels.

Lokapure and Joshi [9] focused on the issue of retaining the Energy released to the hot warehouse from the cold warehouse of the air conditioning system. This waste energy is considered waste Energy to increase the performance coefficient of the system. It was found that the actual improvement of this coefficient reached (13.66%); however, it

reached the planned increase, which is (20%). Also, the investment in this wasted energy has reduced thermal pollution.

Therefore, sympathetic to the issue of recovering waste heat from machines subject to the laws of thermodynamics, in this current paper, the performance of the ordinary solar distiller combined with the waste hot air emitted from the air conditioning system condenser and dispersed to the heat sink (which represents the atmospheric environment) will be theoretically analyzed, according to the climatic conditions of the Nasiriyah district located in southeastern Iraq (31.0538°N (latitude), 46.267°E (longitude)).

## 2. Description and physical principle of the hybrid desalination rig

The physical principle of the solar distiller system alone (passive type) is summarized in the evaporation and condensation processes. The proposed model for this study is a solar distillation system with a single inclination of its glass cover, with the inner part of this system painted black, as in Fig.1. Heat transfer occurs due to the heat emitted by the black body to the low salty water layer. The source of this heat emitted by the black body is due to the heat it absorbs from the solar radiation. This layer of water is heated to the point where it generates steam, which rises to the top and condenses on the surface of the lid glass in the form of very pure water droplets. It is required if the dew point of the water vapour formed is greater or equal to the temperature of the glass cover.

It has been assumed that there is an additional thermal enhancement in addition to the heat generated by the effect of solar radiation, as they improve the internal heat exchange of the solar distiller system.

The enhancement occurs during the current study from the heat emitted by the condenser of the cycle (vapour compression cycle), which is considered a heat sink for the air conditioning unit system according to the laws of thermodynamics.

The heat from the condenser is directed into the basin of the solar distiller through two heat exchangers. The first receives heat from the condenser to give it to the other exchanger immersed within the surface layer of salt water in a closed thermodynamic cycle. The source of feeding these two heat exchangers with the water used to heat the submerged exchanger tubes differs from that of feeding the salt water layer inside the system basin. The water is circulated between the two exchangers through a suitable thrust pump.

The immersed heat-exchanger in the brine layer works as a thermal storage heater for the water, to raise the surface temperature of the brine, so the difference between the temperature of the glass cover and the dew point of the water vapor becomes greater, thus increasing the amount of heat flux required for evaporation, thus increasing the amount of pure water productivity, (see Fig.1).

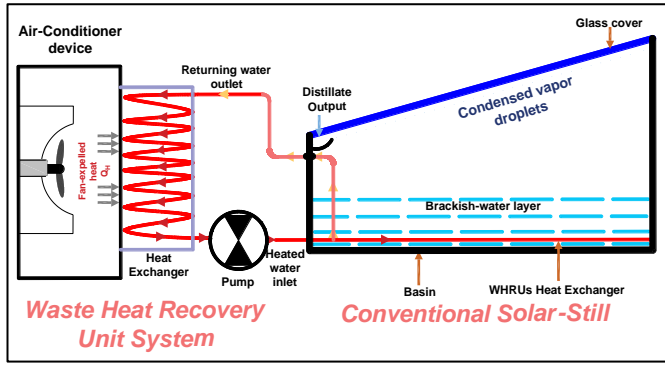


Fig.1 The physical descriptive model.

### 3. Theoretical Analysis

The significant assumptions will be followed to simplify the mathematical model:

1. The transmittance of the glass lid and brackish-water layer is perfect.
2. The uniform temperature of the glass lid.
3. The solar distillation system is completely sealed from leaking water vapour and in a quasi-steady state.
4. There are no heat losses from the base and sides basin.
5. One-dimensional heat transfer model.
6. The thermodynamic cycle of the closed type of the WHRU<sub>s</sub>.

#### 3.1 Balancing the energies of the passive solar distiller

The heat exchange that occurs from and to the basin of the solar distiller system is due to two reasons: First, internal heat transfer within the basin cabin by (convection, evaporation, and radiation), and from the black basin to the brackish water layer. Second, ambient heat transfer (from the glass lid to the ambient by radiation and convection).

The energy balance equations of the solar distiller are given in terms of heat transfer co-efficient as [10] (see Fig.3):

##### • For Basin:

$$(q_{so.})_b = q_{bw} + q_b \quad (1)$$

$$\alpha_b \cdot I_T = h_{bw}(T_b - T_w) + h_b(T_b - T_\infty) \quad (2)$$

##### • For brackish water layer:

$$(q_{so.})_w + q_{bw} + q_{H.E} = (q_{cw} + q_{ew} + q_{rw}) + q_{st}. \quad (3)$$

$$\alpha_w \cdot I_T + h_{bw}(T_b - T_w) + (m \cdot C_p)_w(T_i - T_o) = (h_{1w}) \cdot (T_w - T_g) + (M \cdot C_p)_w \cdot \frac{dT_w}{dt} \quad (4)$$

##### • For Glass lid:

$$(q_{so.})_g + (q_{cw} + q_{ew} + q_{rw}) = (q_{cg} + q_{rg}) \quad (5)$$

$$\alpha_g \cdot I_T + h_{1w}(T_w - T_g) = h_{1g}(T_g - T_\infty) \quad (6)$$

#### 3.1.1. Coefficients of the heat transfer

The total internal heat transfer coefficients from the brackish water layer to the layer of glass lid can be calculated as [11]:

$$h_{1w} = h_{cw} + h_{ew} + h_{rw} \quad (7)$$

Where the convection, evaporation, and radiation heat transfer coefficients are expressed as [11]:

$$h_{cw} = 0.884 \cdot \sqrt[3]{T_w - T_g + \frac{(P_w - P_g) \cdot T_w}{268900 - P_w}} \quad (8)$$

$$h_{ew} = 0.016273 h_{cw} \cdot \frac{P_w - P_g}{T_w - T_g} \quad (9)$$

$$h_{rw} = \sigma * [-1 + \varepsilon_g + \varepsilon_w]^{-1} * (T_w + T_g) \cdot [T_w^2 + T_g^2] \quad (10)$$

The saturated vapour pressure at the brackish-water layer and glass lid in equations (8,9) is expressed as follows [12]:

$$P_w = e^{25.317 - (5144/T_w)} \quad (11)$$

$$P_g = e^{25.317 - (5144/T_g)} \quad (12)$$

The total heat transfer coefficients by convection and radiation from glass lid to ambient ( $h_{1g}$ ), depending on the local wind velocity ( $V_w$ ), is expressed as [10]:

$$h_{1g} = 5.7 + 3.8V_w \quad (13)$$

#### 3.1.2 Solar radiation

The quantity of the incident total solar radiation on the blackbody of the basin solar distiller ( $I_T$ ), which is horizontal, can be calculated from [13]:

$$I_T = I_D \cdot \cos \theta + I_{diff} \quad (14)$$

The incident direct solar radiation ( $I_D$ ) is calculated depending on the altitude angle ( $\varphi$ ):

$$I_D = A \cdot e^{-B/\sin \varphi} \quad (15)$$

$$\varphi = \sin^{-1}(\cos(L) \cdot \cos(D) \cdot \cos(\mathcal{H}) + \sin L \cdot \sin D) \quad (16)$$

The altitude angle ( $\varphi$ ) depends on the local latitude ( $L$ ), hour ( $\mathcal{H}$ ), declination ( $D$ ) angles, which can be expressed according to the local o'clock time ( $t$ ), and the date sequence number of the specified day of the year [14]:

$$\mathcal{H} = 15^\circ \cdot (t - 12) \quad (17)$$

$$D = 23.5 \sin[0.986(d + 284)] \quad (18)$$

The diffuse solar radiation ( $I_{diff}$ ) is calculated depending on the amount of incident direct solar radiation ( $I_D$ ), [15]:

$$I_{diff} = C \cdot I_D \quad (19)$$

The angle of incidence of the solar rays ( $\theta$ ) is expressed as follows [13]:

$$\theta = \cos^{-1}(\sin(\varphi)) \quad (20)$$

Where (A, B, and C) are constants, their values are shown in Fig.1, according to the sequence of the month of the year.

Constants for ASHRAE equations for the average values of each month			
Months	A, $\text{Wm}^{-2}$	B, dimensionless	C, dimensionless
January 17	1,229.882	0.142	0.058
February 16	1,216.255	0.144	0.060
March 16	1,190.407	0.153	0.068
April 15	1,144.663	0.175	0.092
May 15	1,109.680	0.192	0.116
June 11	1,092.697	0.202	0.130
July 17	1,084.880	0.207	0.136
August 16	1,102.968	0.202	0.124
September 15	1,142.120	0.182	0.098
October 15	1,183.449	0.164	0.077
November 14	1,213.611	0.151	0.065
December 10	1,228.004	0.145	0.059

Fig. 2 Direct solar radiation constants [13].

### 3.1.3 Ambient temperature

The hourly ambient temperature ( $T_{\infty}$ ) throughout the night and daylight, shown in the previous equations, is estimated based on the local daily minimum and maximum climate temperature by utilizing the following formulas [14]:

For daylight:

$$T_{\infty} = (T_{\infty,max} - T_{\infty,min}) \cdot \sin\left(\frac{\pi t}{L_D + 3.6}\right) + T_{\infty,min} \quad (21)$$

For night:

$$T_{\infty} = (T_{\infty,sunset} - T_{\infty,min}) \cdot e^{-2.2 \cdot \frac{t-L_D}{24-L_D}} + T_{\infty,min} \quad (22)$$

Where the length of daylight ( $L_D$ ) is given based on the hour angle at sunset and sunrise ( $\mathcal{H}_o$ ) by [11]:

$$L_D = \frac{2}{15} \cdot \mathcal{H}_o \quad (23)$$

$$\mathcal{H}_o = \cos^{-1}(-\tan(\mathcal{L}) \cdot \tan(\mathcal{D})) \quad (24)$$

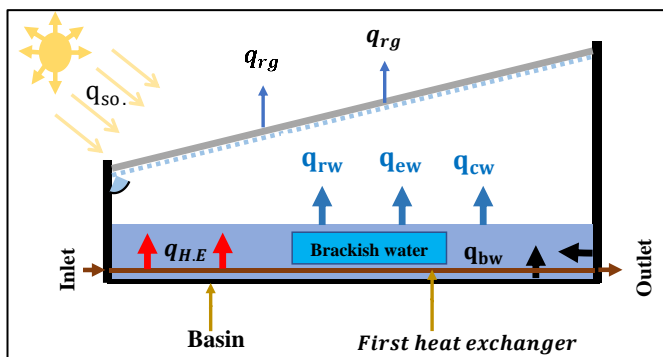


Fig. 3 Energy balance of the hybrid solar-still rig.

### 3.1.4. Brackish-water, glass lid, and absorber temperatures

By equating the values of ( $\alpha_g$ ) and ( $\alpha_{wa}$ ) to zeros, it can be calculated the glass lid temperature ( $T_g$ ) from equation (6) to obtain:

$$T_g = \frac{h_{1w} \cdot T_w + h_{1g} \cdot T_{\infty}}{h_{1w} + h_{1g}} \quad (25)$$

Because there is no heat loss from the sides and the base of the system basin due to the existence of the isolation area, there is no temperature gradient across the insulation wall, so the temperature of the basin and the ambient temperature are almost equal, where ( $T_b = T_{\infty}$ ), to become:

$$T_b = \frac{\alpha_b \cdot I_T}{h_{bw}} + T_w \quad (26)$$

By Substituting equation (14) in equation (26) and equations (25, 26) in equation (4) to obtain the following differential equation:

$$\frac{dT_w}{dt} = f(t_n, T_{w_n}) \quad (27)$$

$$f(t_n, T_{w_n}) = \frac{1}{(M \cdot C_P)_w} \cdot [\alpha_b \cdot I_T - h_{1w} \cdot T_{w_n} + \frac{h_{1w} \cdot T_{w_n} + h_{1g} \cdot T_{\infty}}{h_{1w} + h_{1g}} \cdot h_{1w}] \quad (28)$$

The mass of water in a state of the passive solar distiller is given based on the thickness of the brackish-water layer ( $x$ ) at the bottom of the basin by:

$$M_w = (\rho \cdot A \cdot x)_w \quad (29)$$

### 3.2 Heat transfer by heat exchanger of the WHRU<sub>s</sub>

The conventional solar distiller and waste heat recovery systems from the air conditioning unit condenser represent the hybrid solar distiller. The ( $q_{H.E}$ ) which is the amount of heat acquired by the salt water layer from the first heat exchanger due to the difference between the heat exchanger's entry temperature ( $T_i$ ) and its exit temperature ( $T_o$ ), it can be given as:

$$q_{H.E} = (m \cdot C_P)_w (T_i - T_o) \quad (30)$$

The mass of water in a state of complete adhesion of the heat-exchanger to the bottom of the rig basin, calculated from:

$$M_w = (\rho \cdot A \cdot x)_w - (\rho \cdot A_c \cdot L)_{tube} \quad (31)$$

To solve the differential equations (27) and extract the temperature values ( $T_w$ ,  $T_g$  and  $T_b$ ), this equation must be solved numerically by using the Euler method known for solving differential equations and using the MATLAB program version (R2019a), for the two periods, firstly, from sunrise until sunset and then, secondly, from the time that sunset until the sunrise of the next day. With the interval of (600 seconds), according to the following equations:

$$T_{w_{n+1}} = T_{w_n} + S \cdot f(t_n, T_{w_n}) \quad (32)$$

By using the initial conditions at zero time:

$$T_{wa}(0) = T_{wa_0} \quad (33 a)$$

$$T_g(0) = T_{g_0} \quad (33 b)$$

$$T_b(0) = T_{b_0} \quad (33 c)$$

To obtain the hourly productivity can be estimated from the following equations [12]:

$$me_{hr} = \frac{q_{ew}}{h_{fg}} * 3600 \quad (34)$$

$$h_{fg} = 2501.89715 - 2.40706404 * T_w + 1.19222 * 10^{-3} * T_w^2 - 1.5863 * 10^{-5} * T_w^3 \quad (35)$$

And accumulated productivity:

$$me_D = \sum_{i=1}^{24} me_{hr} \quad (36)$$

## 4. Results and discussion

The solar distiller's mathematical representation has been utilized, and three situations have been theoretically examined. The First Period, which includes the case of the conventional desalination rig during the night period from (00:00-  $t_{\text{sunrise}}$ ) with the presence of (WHRUs) as a heat source. The Second Period includes the case of the conventional desalination rig during the day, relying on solar radiation as a heat source, and in the absence of (WHRUs), from ( $t_{\text{sunrise}}$ - $t_{\text{sunset}}$ ). As for the third period, it operates during the remainder of that day in the absence of the sun and relies on the (WHRUs) system as a source of heat ( $t_{\text{sunset}}$  -24:59:59), for different months.

Version (R2019a\_9.6.0.1072779) of the MATLAB programming language was used for all calculations. The values of the design parameters for the two systems, waste heat recovery from an air conditioner condenser device and solar distillation, are shown in Table (1). The surface temperature of the evaporating water in the basin of the solar distiller can be evaluated by using Euler's approach, which is effective for solving first-order differential equations

### 4.1. Sunlight radiation fluctuation

Fig.4 depicts the average solar radiation intensity that fell on the conventional solar-still system's basin throughout the year's summer months. It reveals that the maximum intensity was calculated theoretically in June, reaching ( $1040.81 \text{ W/m}^2$ ) at hour midday noon, while the lowest value calculated was in August, reaching ( $965.246 \text{ W/m}^2$ ) for the same local time. The cause of this is due to the disparity in the declination angle of the solar rays ( $D$ ) for each day of the year, in addition to the variation in the altitude angle ( $\varphi$ ) due to the disparity in the hour-angle ( $\mathcal{H}$ ).

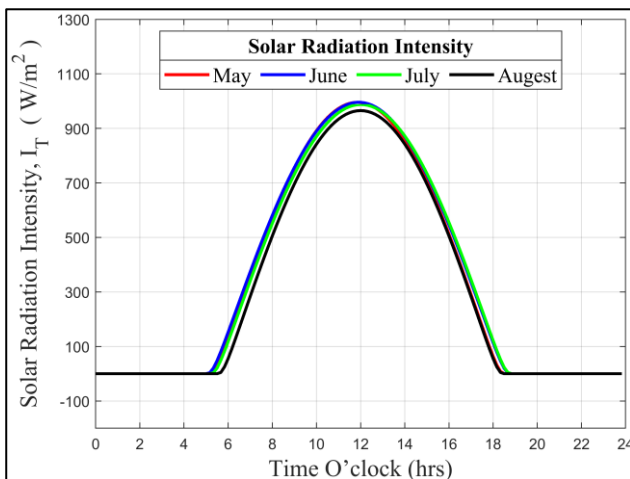


Fig.4 The variation of solar radiation intensity for the summer months.

### 4.2. Temperature variation

It has been observed from the temperature charts (see Fig.6) (for the second period - the daytime period) from the results of the theoretical model that by neglecting the absorption of solar radiation by the surface of the basin water and the glass cover, relying only on what is absorbed by the black body of the base of the stationary solar basin - according to the assumptions made in the introduction to this current study - that the surface temperature of the basin water exceeds the temperature of the glass cover by a good percentage, which gives a high evaporation rate and a good amount of condensation that generates clean water droplets. The temperature of the black body basin of the desalination system also exceeds the temperature of the saline basin water, which increases the quality of the amount of convection heat transfer from the base basin to the brine layer.

As for the first and third periods of the night, it was noticed that the temperature rising coming out of the condenser of the air conditioning unit raises the temperature of the saltwater layer of the traditional desalination basin, which increases the difference between it and the temperature of the glass cover, which makes evaporation more. Also, during these two periods, it was got the attention that the temperature of the salty water layer of the basin ( $T_w$ ) was significantly higher than the temperature of the base of the black body basin ( $T_b$ ), and this is the opposite of what happens to the desalination system during exposure to solar radiation (during the day).

It is because during the day, the main and only source of heat for evaporation is the solar radiation that is absorbed by the base basin of the desalination system in response to the so-called (black body characteristic), so the base of the basin is the source of heat emission and its transfer to the water layer in contact with the base of the basin with a black body. As for the first and third parts of the night period, the (WHRU) system is connected to the desalination system utilizing a heat exchanger immersed in the basin water layer, and this hot exchanger transfers heat to this layer of water, which in turn transfers heat to the base of the basin.

From Fig.5-A, Fig.5-C, Fig.6-A, and Fig.6-C, it is clear from the first and third periods that despite the absence of solar radiation, the temperature of the basin water ( $T_w$ ) and the temperature of the black basin ( $T_b$ ) begin to rise with time from (00:00) until sunrise, and the higher the temperature of the air expelled from the condenser in the air conditioning unit ( $T_{fan}$ ), the temperature of the ( $T_w$ ) increases, and in turn, raises the temperature of the ( $T_b$ ), which makes the magnitude of ( $T_w - T_g$ ) larger. Then, the temperatures begin to stabilize at (2:00) until they reach sunrise for the first period. In contrast, they stabilize at (20:40) for the third period.

In the case of the day, between the periods of sunrise and sunset, according to Fig.4, which shows the variation in the intensity of solar radiation throughout the total day, the effect of the (WHR) temperature in (Fig.5-B and Fig.6-B) fades away at sunrise, because the amount of heat gained by the basin water layer from the thermal emission of the black body base of the basin due to the higher solar radiation is compared to the amount of heat gained during the two-night periods by (WHRUs). Then, the temperatures began to decline and fall in conjunction with the receding of the solar radiation until it completely disappeared at sunset, and this is evident in Fig.5 and Fig.6.

4.3. Productivity variation

The instantaneous and cumulative productivity in the first period rises at (2:00) and then declines at sunrise due to the atrophy of the effect of (WHRUs). Productivity declines at sunset and gradually rises due to the effect of the (WHRUs), as in figures from (Fig.7-Fig.12).

Table 1. Physical parameters.

Parameter	Value	Unit
$A_b$	1	$m^2$
$A_g$	1	$m^2$
$\alpha_b$	0.5	-
$\alpha_w=\alpha_g$	0	-
$x$	0.015	m
$m_w$	0.00225	Kg/s
$V_w$	3	m/s
$Cp_w$	4200	J/kg K
$Cp_{air}$	1006.9	J/kg K
$h_b$	14	$W/m^2 K$
$h_{bw}$	100	$W/m^2 K$
$\rho_w$	1000	$Kg/m^3$
$\epsilon_w$	0.9	-
$\epsilon_g$	0.88	-
$\sigma$	$5.67 \times 10^{-8}$	$W/m^2 K^4$

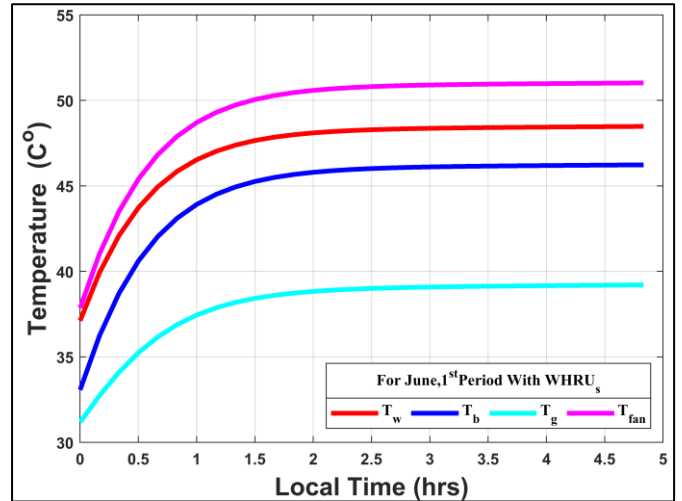
5. Conclusion

During this study, an analysis of the mathematical model was conducted to improve the performance of passive solar distillers operating during the day, when connected to the waste heat recovery system (WHRUs) from the condenser of the air conditioning unit, operating at night, by changing the temperature of ( $T_{fan}$ ) that enters the heat exchanger placed on the base of the basin of the conventional desalination system. The following conclusions were reached:

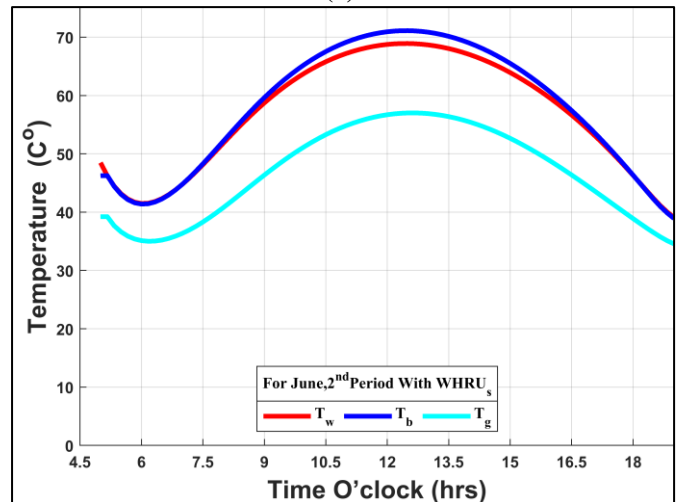
1. The largest hourly productivity obtained was (0.31 kg/hr) during the second period in June.
2. The largest instantaneous hourly productivity was obtained during the night hours during the first and third periods combined, and that was in the month of (July) with an amount of (0.1452 kg/hr).
3. The largest cumulative productivity is evident in Table 2.
4. The rate of improvement of the system, in general, was (29.935-31.907%).
5. The performance improvement rate for four months was (30.28 %).
6. This study is limited to the season where the air conditioning unit is used, namely in the summer.

Table 2. Accumulated productivity rate and percentage of improvement by WHRU<sub>s</sub>, for different months.

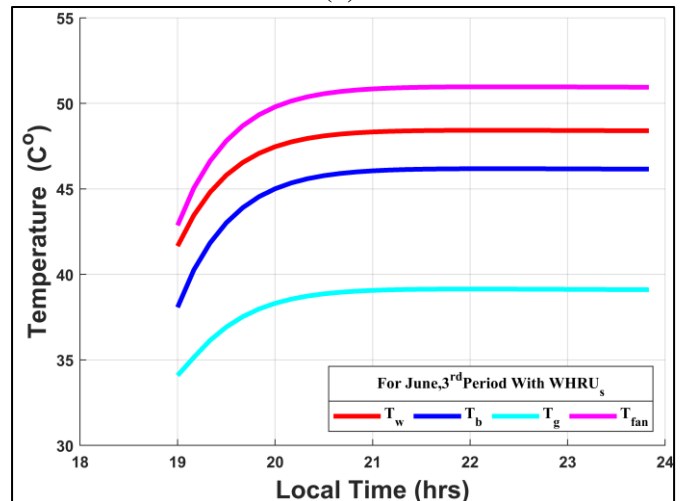
Month	1 <sup>st</sup> Period	2 <sup>nd</sup> Period	3 <sup>rd</sup> Period	% Improvement
May	1.0531	4.7934	0.99484	29.935
June	1.0225	5.0887	1.051	28.951
July	1.0439	4.8638	1.0733	30.328
August	1.0593	4.5848	1.089	31.907



(a)

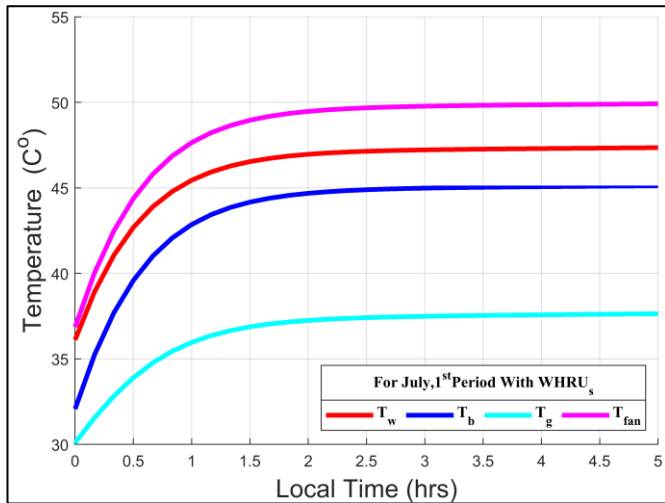


(b)

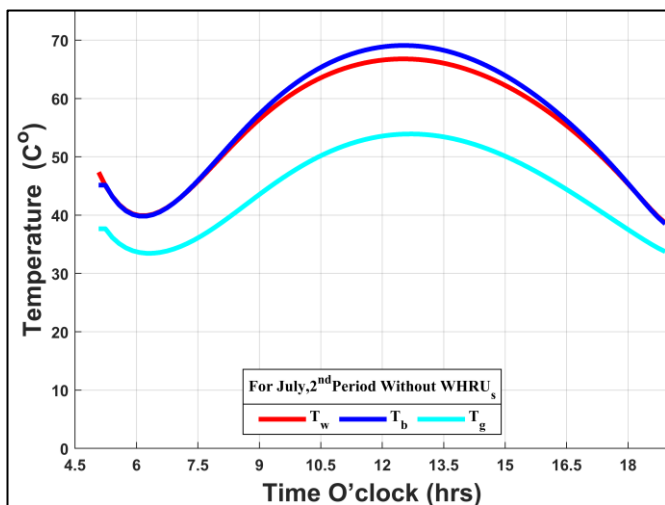


(c)

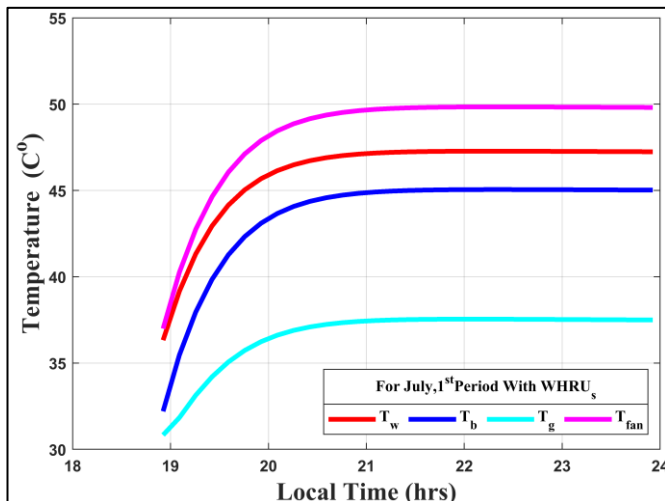
Fig. 5 Water, basin, glass, and ejected to the ambient temperatures variation with time for June, (A) and (C) during the night, while (B) during the light day.



(A)

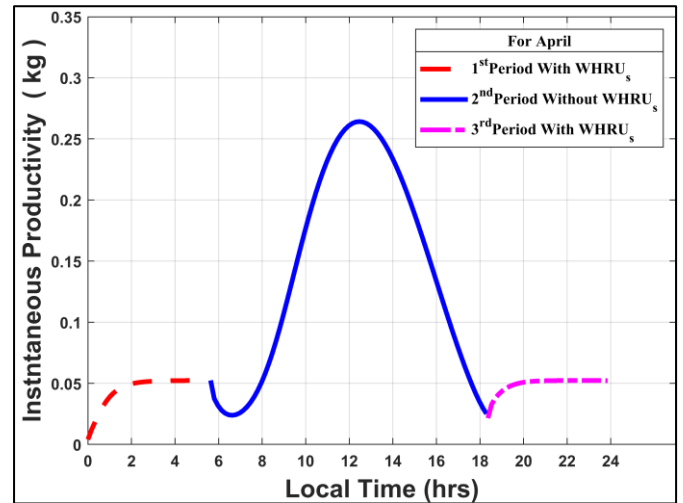


(B)

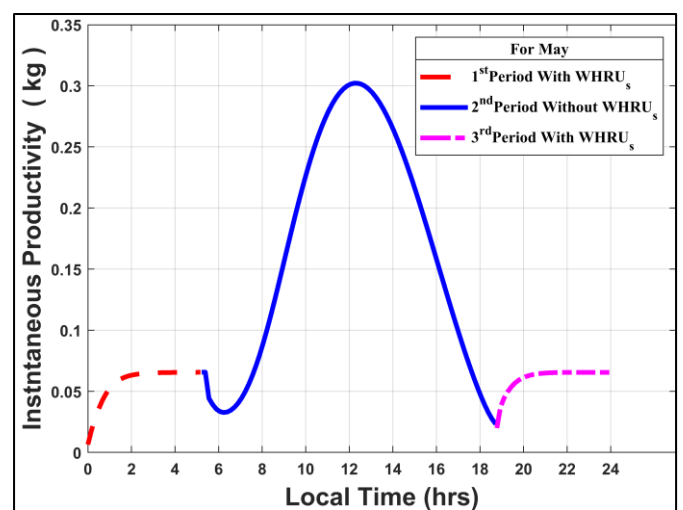


(C)

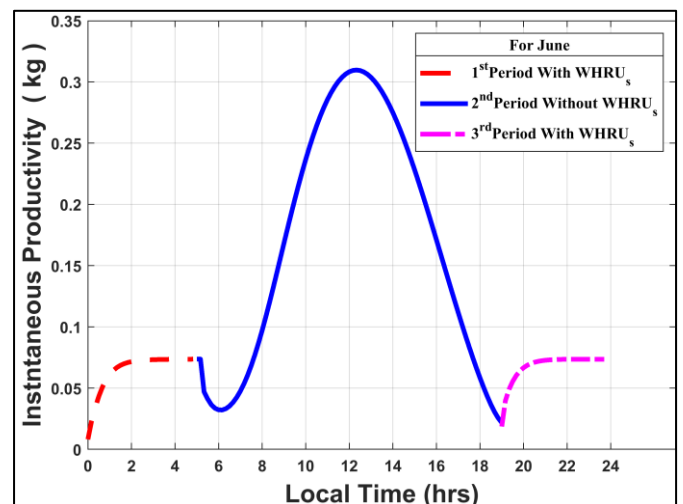
**Fig. 6** Water, basin, glass, and ejected to the ambient temperatures variation with time for July, (A) and (C) during the night, while (B) during the light day.



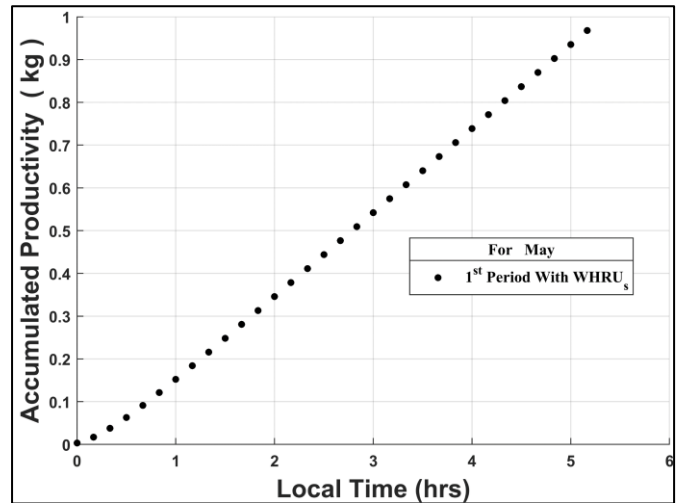
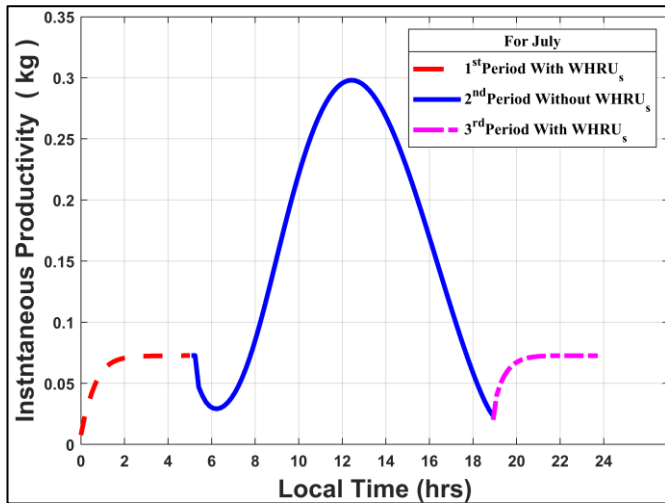
**Fig. 7** Effect of the (*WHRUs*) on the instantaneous productivity during the night for April.



**Fig. 8** Effect of the (*WHRUs*) on the instantaneous productivity during the night for May.

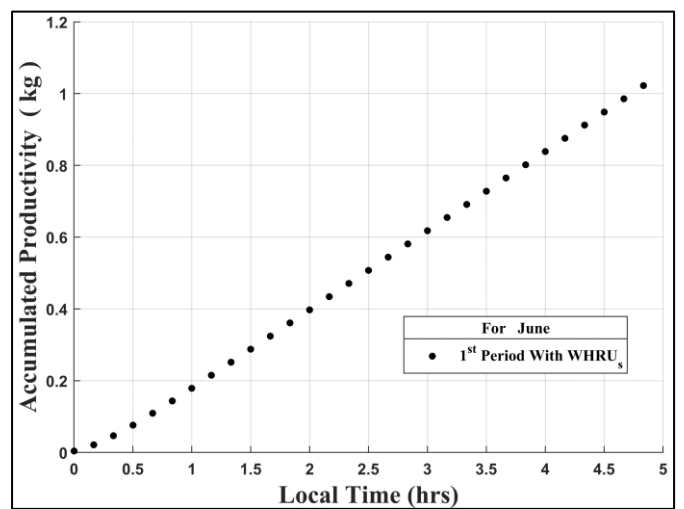
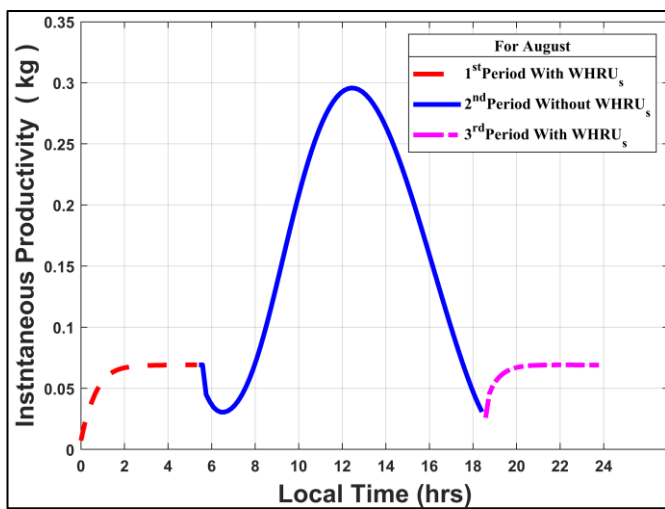


**Fig. 9** Effect of the (*WHRUs*) on the instantaneous productivity during the night for June.



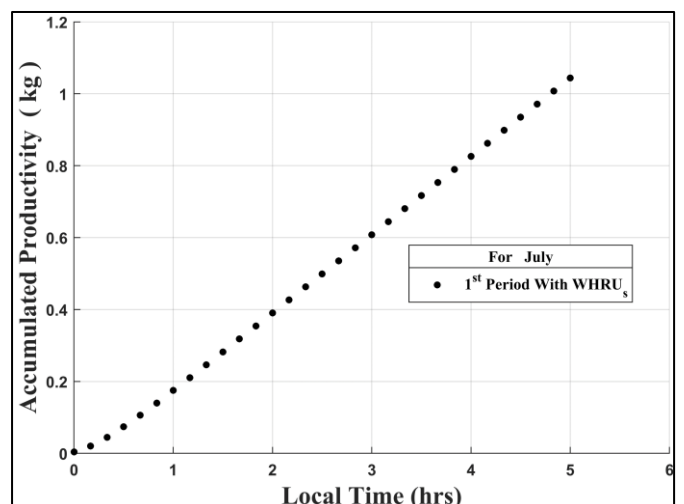
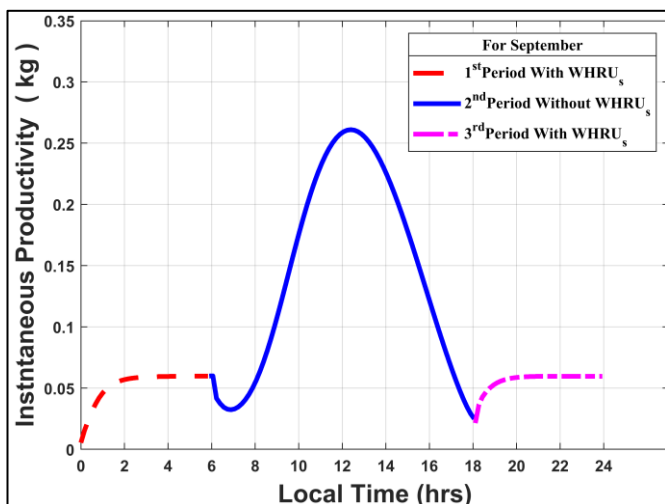
(A)

Fig. 10 Effect of the ( $WHRU_s$ ) on the instantaneous productivity during the night for **July**.



(B)

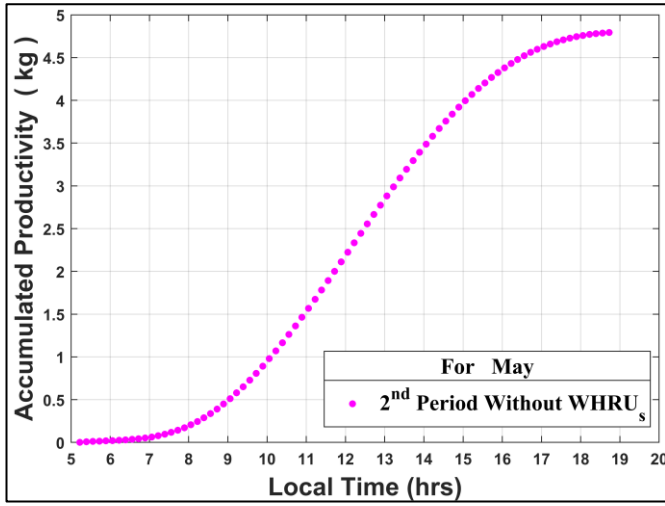
Fig. 11 Effect of the ( $WHRU_s$ ) on the instantaneous productivity during the night for **August**.



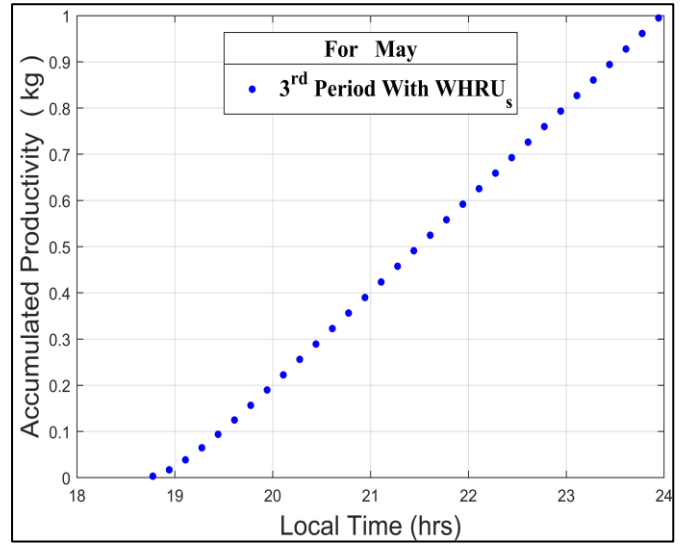
(C)

Fig. 12 Effect of the ( $WHRU_s$ ) on the instantaneous productivity during the night for **September**.

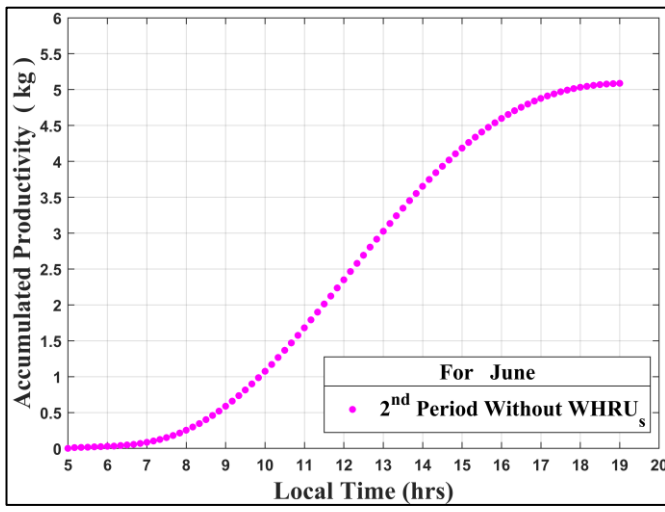
Fig. 13 shows the results of the accumulative output of the first period for different months.



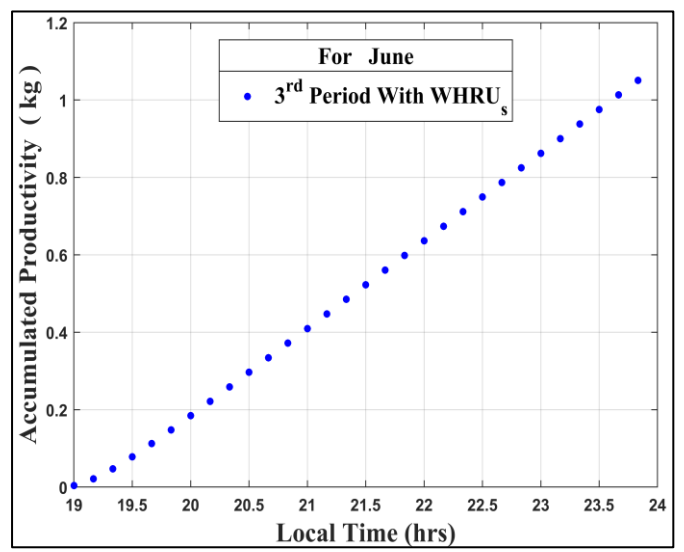
(A)



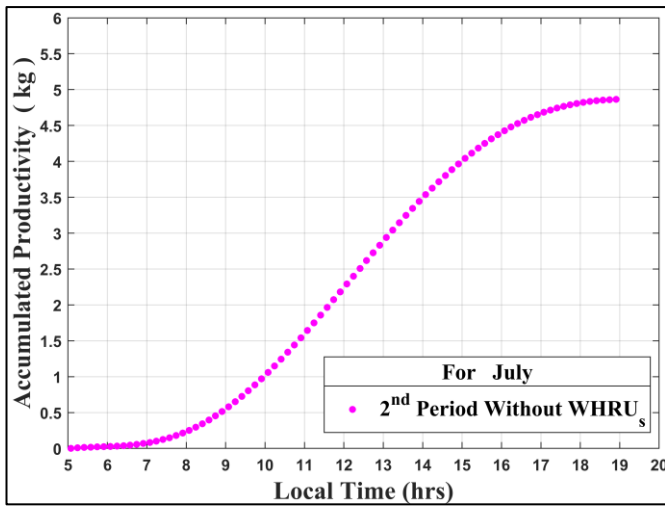
(A)



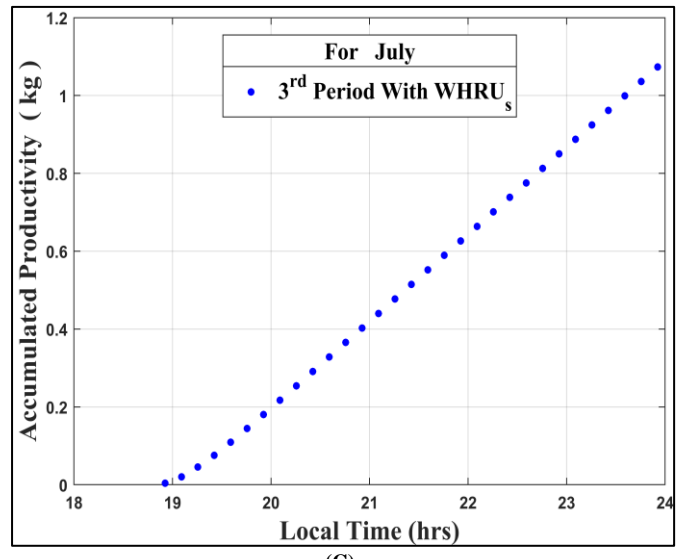
(B)



(B)



(C)



(C)

Fig. 14 shows the results of the accumulative output of the second period for different months.

Fig. 15 shows the results of the accumulative output of the third period for different months.

Nomenclature		
Symbol	Description	Unit
$I_D$	Direct solar-radiation intensity	W/m <sup>2</sup>
$I_{diff}$	Diffusion solar-radiation intensity	W/m <sup>2</sup>
$I_T$	Total solar-radiation intensity	W/m <sup>2</sup>
$d$	No. of the days of the year from 1 <sup>st</sup> , Jan.	Day
$L_D$	The length of light day	hrs.
$L_{tube}$	The length of the heat exchanger	m
$M$	Mass of brackish-water layer	kg
$h_b$	Heat transfer coefficient from basin to ambient	W/m <sup>2</sup> K
$h_{cw}$	Convection heat transfer coefficient from water to glass cover	W/m <sup>2</sup> K
$h_{ew}$	Evaporation heat transfer coefficient from water to glass cover	W/m <sup>2</sup> K
$h_{rw}$	Radiation heat transfer coefficient from water to glass cover	W/m <sup>2</sup> K
$h_{cg}$	Convection heat transfer coefficient from glass cover to ambient	W/m <sup>2</sup> K
$h_{rg}$	Radiation heat transfer coefficient from glass cover to ambient	W/m <sup>2</sup> K
$P_w$ and $P_g$	Saturated vapour pressure at the water layer and glass cover temperature	N/m <sup>2</sup>
$q_{bw}$	Heat flux from basin to water	W/m <sup>2</sup>
$q_{cw}$	Convection heat transfer from water to glass cover	W/m <sup>2</sup>
$q_{ew}$	Evaporation heat transfer from water to glass cover	W/m <sup>2</sup>
$q_{rw}$	Radiation heat transfer from water to glass cover	W/m <sup>2</sup>
$q_{cg}$	Heat loss from glass to ambient by convection	W/m <sup>2</sup>
$q_{rg}$	Heat loss from glass to ambient by radiation	W/m <sup>2</sup>
$q_b$	Heat loss from basin to ambient	W/m <sup>2</sup>
$q_{st.}$	The rate of heat storage	W/m <sup>2</sup>
$t$	Time	Seconds
$V_w$	Velocity wind	m/s
$T_\infty$	Ambient temperature	°C
$T_b$	Basin temperature	°C
$T_g$	Glass cover temperature	°C
$T_w$	Brackish water temperature	°C
$T_{fan}$	Expedled condenser of A/C temperature	°C
$T_i$ and $T_o$	Inlet and outlet temperature of heat exchanger	°C
$T_{\infty, sunset}$	The ambient temperature at sunset	°C
$D$	Declination angle	degree
$\mathcal{H}$	Hour angle	degree
$\mathcal{H}_o$	Hour angle at sunrise and sunset	degree
$\mathcal{L}$	Latitude angle	degree
$\varphi$	Altitude angle	degree
$\theta$	Incident angle	degree
$WHRU_s$	The waste heat recovery system of A/C	-

## References

- [1] D. W. Rufus, S. Iniyan, L. Suganthi, and P. A. Davies, "Solar stills: A comprehensive review of designs, performance, and material advances", *Renewable and sustainable energy reviews*, Vol. 63, pp. 464-496, 2016. <https://doi.org/10.1016/j.rser.2016.05.068>
- [2] S. N. Rai and G. N. Tiwari, "Single basin solar still coupled with flat plate collector", *Energy Conversion and Management*, Vol. 23, pp. 145-149, 1983. [https://doi.org/10.1016/0196-8904\(83\)90057-2](https://doi.org/10.1016/0196-8904(83)90057-2)
- [3] G. N. Tiwari, S. K. Shukla, and I. P. Singh, "Computer modelling of passive/active solar stills by using inner glass temperature", *Desalination*, Vol. 154, Issue 2, pp. 171-185, 2003. [https://doi.org/10.1016/S0011-9164\(03\)80018-8](https://doi.org/10.1016/S0011-9164(03)80018-8)
- [4] A. Sh. Sadiq, "Artificial Neural Network for Evaluating the Performance of a Solar Still Using a Heating Pipe Evacuated Tubes Collector", University of Basrah, Basrah, Iraq, 2014.
- [5] K. Y. Mahammed, R. Kerfah, and M. Bezzina, "Improving the water production of a solar still by adding an internal condensation chamber: A theoretical study", *Environmental Progress & Sustainable Energy*, Vol. 38, Issue 5, 2019. <https://doi.org/10.1002/ep.13198>
- [6] Z. S. Abdel-Rehim and A. Lasheen, "Improving the performance of solar desalination systems", *Renew Energy*, Vol. 30, Issue 13, pp. 1955-1971, 2005. <https://doi.org/10.1016/j.renene.2005.01.008>
- [7] S. K. Singh, S. K. Tyagi, and S. C. Kaushik, "Desalination Using Waste Heat Recovery with Active Solar Still", the 7th International Conference on Advances in Energy Research, 2020.
- [8] A. Shafieian and M. Khiadani, "A multipurpose desalination, cooling, and air-conditioning system powered by waste heat recovery from diesel exhaust fumes and cooling water", *Case Studies in Thermal Engineering*, Vol. 21, 2020. <https://doi.org/10.1016/j.csite.2020.100702>
- [9] R. B. Lokapure and J. D. Joshi, "Waste heat recovery through air conditioning system", *International Journal of Engineering Research and Development*, Vol. 5.3, pp. 87-92, 2012.
- [10] S. H. Hammadi, "Combined Solar Chimney Power Plant and Solar Still", *Basrah Journal for Engineering Science*, Vol. 16, Issue 2, pp. 100-107, 2016.
- [11] S. H. Hammadi, "Integrated solar still with an underground heat exchanger for clean water production", *Journal of King Saud University - Engineering Sciences*, Vol. 32, Issue 5, pp. 339-345, 2020. <https://doi.org/10.1016/j.jksues.2019.04.004>
- [12] D. W. Medugu and L. G. Ndatuwong, "Theoretical analysis of water distillation using solar still", *International Journal of Physical Sciences*, Vol. 4, Issue 11, pp. 705-712, 2009.
- [13] K. Bakirci, "Estimation of Solar Radiation by Using ASHRAE Clear-Sky Model in Erzurum, Turkey", *Energy Sources, Part A*, Vol. 31, Issue 3, pp. 208-216, 2009.
- [14] S. H. Hammadi, "Freshwater production by combination of solar still, earth-air heat exchanger and solar chimney for natural air draft", *International Journal of Sustainable Engineering*, Vol. 14, Issue 5, pp. 921-932, 2021. <https://doi.org/10.1080/19397038.2021.1941392>
- [15] G. N. Tiwari and L. Sahota, *Advanced Solar-Distillation Systems Basic Principles, Thermal Modeling, and Its Application*, vol. 10. Green Energy and Technology, 2017. ISBN 978-981-10-4672-8 <https://doi.org/10.1007/978-981-10-4672-8>